NJC

Accepted Manuscript

This is an *Accepted Manuscript*, which has been through the Royal Society of Chemistry peer review process and has been accepted for publication.

Accepted Manuscripts are published online shortly after acceptance, before technical editing, formatting and proof reading. Using this free service, authors can make their results available to the community, in citable form, before we publish the edited article. We will replace this *Accepted Manuscript* with the edited and formatted *Advance Article* as soon as it is available.

You can find more information about *Accepted Manuscripts* in the Information for Authors.

Please note that technical editing may introduce minor changes to the text and/or graphics, which may alter content. The journal's standard Terms & Conditions and the Ethical guidelines still apply. In no event shall the Royal Society of Chemistry be held responsible for any errors or omissions in this *Accepted Manuscript* or any consequences arising from the use of any information it contains.

ROYAL SOCIETY OF CHEMISTRY

www.rsc.org/njc

Journal Name

ARTICLE

Synthesis and characterization of tributyl phosphate grafted carbon nanotubes by floating catalytic chemical vapor deposition method and their sorption behavior towards Uranium

Shruti Mishra[a,b], Jaya Dwivedi[b], Amar Kumar[c] and Nalini Sankararamakrishnan[a*]

Received 00th January 20xx,
Accepted 00th January 20xx

DOI: 10.1039/x0xx00000x

www.rsc.org/

Abstract

Carbon nano tubes (CNTs) were synthesized by floating catalytic chemical vapor deposition technique using ferrocene and benzene as the hydrocarbon source. Functionalization of CNts were carried out by oxidation (CNT-OX) and grafting with tributyl phosphate (TBP) ligand (CNT-TBP). Various spectroscopic techniques including Scanning electron microscopy (SEM), Fourier transform Infra red Spectroscopy (FTIR), BET surface area and X-ray photoelectron spectroscopy (XPS) were used to characterize the adsorbents. FTIR and XPS studies revealed the efficient grafting of TBP ligand on the CNT surface. Effect of initial pH and contact time for maximum adsorption of U(VI) with CNT-Plain, CNT-OX and CNT-TBP were studied. The spontaneity of the sorption was confirmed by thermodynamic data. A Pseudo Second Order model with a regression coefficient > 0.978 was obtained for CNT-TBP and equilibrium reached within 3 h. Langmuir maximum adsorption capacity of U(VI) at pH 5 for CNT, CNT-OX and CNT-TBP were found to be 66.6, 100.0 and 166.6 mg/g respectively. Using 0.1 M HCL as desorbent recyclabilioty studies were carried out for three cycles. The probable mechanism of adsorption between U(VI) and CNT-TBP could be understood through FTIR and XPS techniques.

Keywords: Carbon nanotubes, Functionalization, Uranium, Removal, Adsorption

1. Introduction

Advance treatment methods are required for the radio active wastes produced by nuclear power plants [1,2]. Uranium is one of the major waste materials in spent nuclear fuels or mine tailings, and can cause significant contamination[3]. An exposure level of 0.1 mg/Kg of body weight of natural U could result in kidney damage[4]. The World Health Organization's guideline value for uranium is set at 50 µg/L[5]. Several methods have been found useful for the removal of Uranyl ions from process effluents and wastewater. For water treatment, compared to other techniques adsorption has been found to be a preferred technique owing to the flexibility, cost effectiveness, ease of

[a] Centre for Environmental Science and Engineering, Indian Institute of Technology Kanpur, Kanpur, U.P. 208016, India
[b] Department of Chemistry, Banasthali Vidyapith, Rajasthan 304022, India
[c] Bhabha Atomic Research Centre, Trombay, Mumbai, India
* Author for correspondence, +915122596360, nalini@iitk.ac.in

operation and simple design. A weak affinity and low adsorption capacity are exhibited by natural adsorbents for U(VI) under ambient conditions. Therefore, there is need for new, eco-friendly and economical adsorbents with high adsorption capacities and stronger chemical interaction towards U(VI). Among the various adsorbents reported in literature, sorption materials made of Carbon offer variety of advantages including high thermal and radiation resistance and improved chemical stability in acidic conditions compared to other inorganic sorbents and ion exchange resins[6]. Various carbonaceous materials like activated carbon[7,8], activated carbon fibers[9], carbon nanotubes[10,11] and mesoporous carbon[12] have been reported for the removal of U(VI) ions from aqueous solution. Tributyl phosphate (TBP) is one of the widely used extractant for the removal of U(VI)[13]. Thus, in this work three kinds of carbon nanotubes namely plain CNTs, oxidized CNTs and TBP grafted CNTs will be prepared structurally characterized by various techniques and would be evaluated for the removal and recovery of U(VI). Using spectroscopic tools the adsorption mechanism between U(VI) and CNT-TBP will also be discussed.

2. Materials and Methods

All reagents and chemicals like nitric acid (HNO_3), sodium hydroxide (NaOH), tributyl phosphate (TBP), uranyl(VI) nitrate ($UO_2(NO_3)_2.6H_2O$), solvents (ethanol, acetone) and other reagents used in this study are of analytical grade. Using Milli-Q purified water (resistivity > 18.2 MΩ cm) the reagents and standards were prepared.

2.1 Preparation of Carbon nanotubes

Carbon nanotubes were prepared by floating catalyst horizontal chemical vapour deposition technique using 2% ferrocene in benzene as the hydrocarbon source[14]. The flow rate of ferrocene/benzene solution and nitrogen gas was controlled by peristaltic pump and mass flow controller (Bronkhorst high-tech. Netherland), respectively. The temperature of the electric furnace was gradually increased to 800°C in nitrogen atmosphere. The flow rate of ferrocene/benzene solution and nitrogen gas was set to 1 ml/min and 100 sccm respectively and the ferrocene/benzene solution was pumped into the reactor for 30 min at 800°C reactor temperature. The reactor was gradually cooled to room temperature. The deposited CNTs were removed and used for further experiments.

2.2 Preparation of CNT-OX

Around 1 gram of plain CNT was heated with 10 ml of nitric acid at 80◦C until the acid evaporated completely. Then, thorough washing with distilled water was carried until pH of filtrate becomes neutral. Finally, the obtained product was dried in the oven at 70 °C for overnight and used for further experiments.

2.3 Preparation of CNT-TBP

One gram of CNT-OX was treated with 20 mL of tri butyl phosphate and the solution was sonicated for 24 h. Then, the obtained mixture was washed with distilled water and dried at 70°C for overnight and used for further experiments.

The preparation of CNT-OX and CNT-TBP is shown in scheme 1.

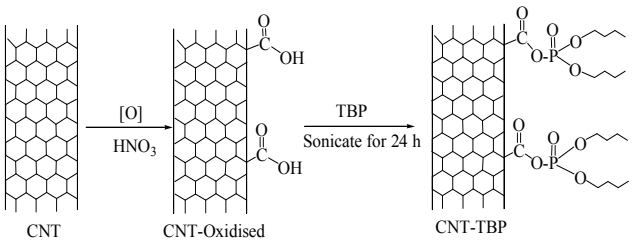

Scheme 1. Preparation of CNT-OX and CNT-TBP

2.4 Batch Studies

Using batch mode, sorption experiments were carried out by equilibrating 20 mL of 100 mg L^{-1} of uranyl ions at pH 5 for 3 h using 0.05 g of the adsorbent. The concentration of uranyl ions in the aqueous phase was analyzed by inductive coupled plasma-mass spectrometry (ICP-MS) (Thermo Scientific, XSERIES 2). The amount of the uranyl ions adsorbed (mg) per unit mass of the adsorbent (g), *qe*, was obtained by the equation given below:

$$qe = \frac{(c_i - c_e)}{m} \times V \qquad (1)$$

Where C_i and C_e are initial and equilibrium concentrations of uranyl ions (mg L^{-1}), V is the volume of the aqueous phase (L), and m is dry mass of the adsorbent (g). Kinetic experiments were conducted by monitoring the amount of uranyl ions adsorbed at regular time intervals. The amount of U(VI) adsorption at temperatures 25˚C, 35˚C and 45˚C were carried out for calculating the thermodynamic parameters. Recyclability of the CNT-TBP was performed using 0.1 M HCl as desorber.

2.5 Instrumentation

Fourier Transform Infra-red (FTIR) measurements were recorded on a Tensor 27 (Bruker, Germany) in the attenuated total reflectance (ATR) mode. SEM micrographs were acquired using FEI Quanta 200 machine. TEM analysis was carried on a Technai G2 T-20 (FEI, Eindhoven, Netherlands) transmission electron microscope operated at 200 kV. Using PHI 5000 Versa Prob II,FEI Inc. spectrometer using non monochromatic Al Kα radiation (1486.6 eV) XPS measurements were carried out. Individual spectral peaks were deconvoluted using XPSPEAK41 software. For fitting the spectral region a nonlinear Shirley background subtraction was applied. The surface characteristics of the sorbent namely, pore size distribution (PSD), pore volume and specific surface area were performed by Autosorb-1C instrument (Quantachrome, USA). Finally, concentration of U(VI) in the aqueous solutions were

determined by Inductive Coupled Plasma mass spectroscopy ICP-MS (Thermo, X-Series2).

3. Results and Discussion

As described in the experimental section, initially CNTs were synthesized by floating catalytic chemical vapour deposition method and grafting was carried by oxidation (CNT-OX) and further treatment with tributyl phosphate (CNT-TBP). Thus the prepared adsorbents viz., CNT-Plain, CNT-OX and CNT-TBP were characterized by various techniques including SEM, TEM, BET surface analyzer, FTIR, XPS and evaluated for its applicability towards the removal of uranyl ions.

3.1 Characterization of Adsorbent

3.1.1 Surface morphology using SEM and TEM

SEM images of plain CNT, oxidized CNT, CNT-TBP is shown in Fig. 1 (a), (b), (c) respectively. The diameter and length of the prepared CNTs were found to be in the range of 20 – 80 nm and 1 – 10 µm respectively (Fig. 1a). In CNT-OX (Fig. 1 (b)) exfoliated rope like structures are observed. This could be attributed to the etching of graphitic layers of CNTs during oxidation. After oxidation and grafting TBP ligand (Fig.1c) there was no appreciable difference in the surface characteristics which confirms the minimal damage occurred after grafting with TBP ligand. The HR-TEM image revealed the presence of nanotubes and iron particles located inside the nanotubes (Fig. 2(a)). The corresponding diffraction rings and bright spot on the electron diffraction pattern (Fig. 2(b)) suggest that the obtained CNTs have crystalline Fe particles.

3.1.2 FTIR analysis of the prepared sorbents

FTIR spectra of CNT-Plain, CNT-OX and CNT-TBP are shown in Fig. 3. A broad peak at ~3430 cm^{-1} is the O-H stretch frequency of the hydroxyl group (Fig. 3). The spectra of CNT-OX show the peaks at 1720 cm^{-1} and 1185 cm^{-1} which are associated with the asymmetric C=O and C–O stretching band of the carboxylic acid (–COOH) group[15]. The peak observed at 1574 cm^{-1} is related to the carboxylate anion stretch mode. Spectra of CNT-TBP presents the C–H bond stretching at around 2960 cm^{-1}, due to methyl groups on MWCNTs . The signal at 2852 cm^{-1} can be assigned to the symmetric stretching of –CH2– groups of tributyl phosphate moiety. Further, in CNT-TBP, the P=O stretching vibration, occurred at 1269 cm^{-1}. The P-O-C vibration occurred at 1027 cm^{-1} [16], which prove the grafting of TBP on CNT surface.

3.1.3 Surface area, Porevolume and Pore size Distribution analysis using BET measurements

The surface characteristics of the plain CNTs, CNT-OX and CNT-TBP were obtained by the standard BET method in relative pressure range from 0.05 to 0.35. The nitrogen adsorption desorption isotherm of CNT-Plain is shown in Fig.4. The material exhibited a Type IV behaviour typical of a mesoporous material. The total pore volume, meso and micro and macro pore volumes, were calculated using the Quantochrome's software. Surface characteristics of various sorbents prepared are listed in Table 1. It is evident from the data that the prepared sorbents possessed small pore size and large surface area which leads to strong confinement of the adsorbed analyte onto the surface of the CNTs. Upon oxidation with nitric acid, specific surface area increased from 99.8 $m^2 g^{-1}$ to 111.9 $m^2 g^{-1}$ which could be attributed to the opening of pores. Further CNT-TBP exhibited a marginal decrease in surface area which is due to the anchoring of TBP ligand.

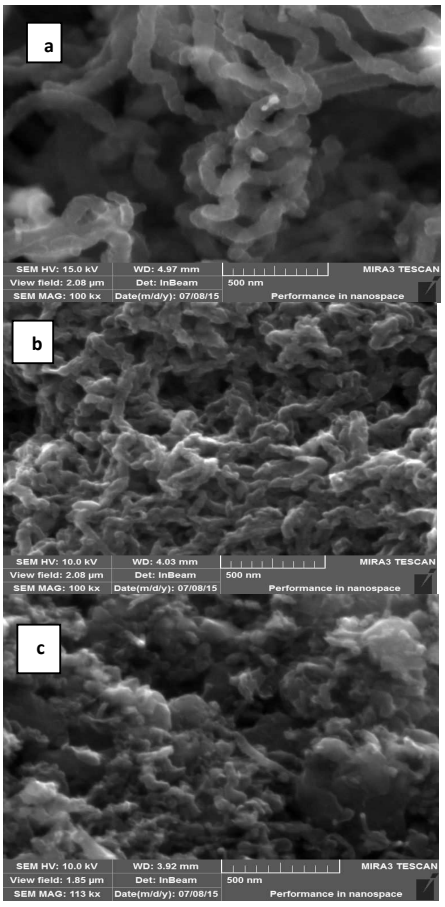

Fig.1 SEM Images of (a) CNT-plain (b) CNT-OX and (c) CNT-TBP

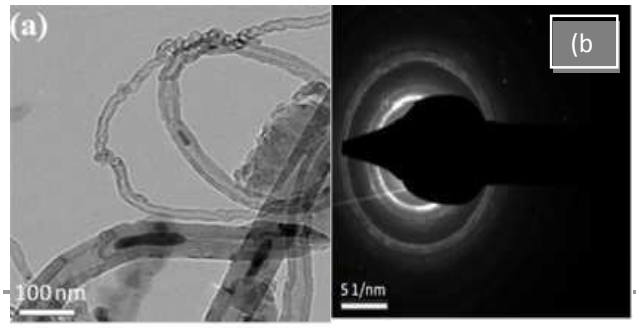

Fig.2 TEM images of CNT-Plain in (a) 100 nm magnification and (b) electronic diffraction spectra

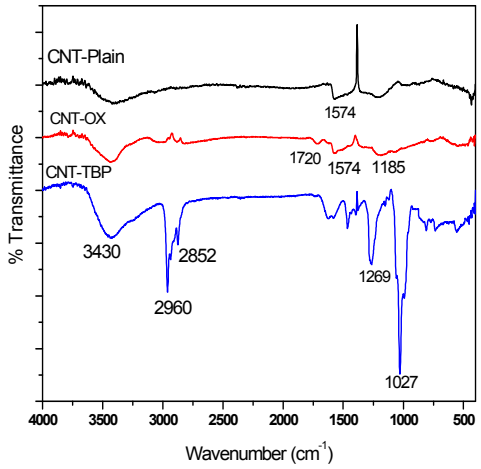

Fig.3 FTIR spectra of CNT-Plain, CNT-OX and CNT-TBP

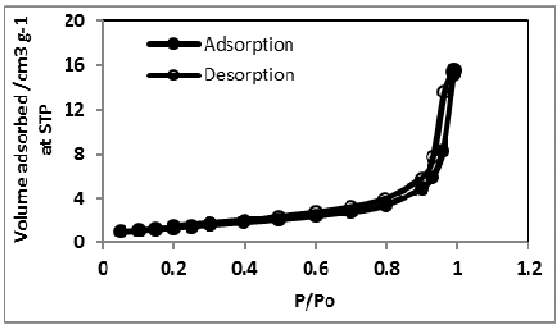

Fig.4 Nitrogen Adsorption Isotherm of CNT-Plain

Table 1. Surface characteristics various prepared CNTs

Adsorbent	Surface Area (m^2/g)	Average Diameter (nm)	Total Pore Volume (cc/g)	Pore volume (cc/g)	
				Meso	Micro
CNT-Plain	99.81	14.67	0.3661	0.4280	0.0048
CNT-OX	111.89	10.52	0.2943	0.1681	0.0049
CNT -TBP	102.77	18.90	0.4861	0.4197	0.0043

3.2 Mechanism of interaction between sorbent and sorbate using XPS and FTIR studies

To study the interaction of U(VI) with CNT-TBP, XPS spectra were recorded for CNT-TB and CNT-TBP-U. Figure 5 illustrates the O 1s, C 1s, P 2p and U 4f spectra. Uranium loading is observed in CNT-TBP-U evidenced by the appearance of doublet peaks of U $4f_{5/2}$ and U $4f_{7/2}$ with a splitting value of 10.72 eV. Table 2 depicts the binding energies of O 1s, C 1s, P 2p and the splitting values of U(VI) spectra. To get a further insight on the U(VI) sorption, the core level scans for C 1s, O 1s, P 2p, and U 4f on CNT-TBP and CNT-TBP-U were analyzed.

The O 1s and C1s spectra of CNT-TBP and CNT-TBP-U are shown in Fig. 6. The peak fitting results of the C 1s, O 1s, P 2p, U 4f, before and after U(VI) loading on CNT-TBP are shown in Table 2. From Fig.6a, the three main components of O 1s spectra occurred at 531.54, 533.56 and 532.87 eV, respectively, corresponding to C=O, O-C=O and C-O-C, C-O-OH, C-OH[17] and C-O-P[18]. Thus the data confirms the grafting of TBP ligand onto CNT surface. After U(VI) loading (Fig 6b) peaks occurred at 531.06, 532.21, 531.76, 532.29 eV. The presence of U=O bond is confirmed by the appearance of additional peak after U(VI) sorption[19,20]. Further after U(VI) adsorption O 1s binding energies shifted to the lower values. This further confirms that complexation occurs between the oxygen-containing tributyl phosphate groups and uranyl ions during adsorption.

Figures 4c and 4d show the molecular level C 1s of CNT-TBP and CNT-TBP-U respectively. The four individual component peaks of C 1s are 284.25, 284.58, 285.06 and 286.03 eV corresponding to C-C, C=C, C-H and C-O-P[17,18] respectively. After uranyl adsorption the peaks shifted to lower binding energies owing to the complexation of tributyl phosphate group and U(VI) ions.

Figures 7a and 7b, denoted the P 2p spectra of CNT-TBP before and after loading U(VI) respectively. In CNT-TBP, the binding energy of $P2p_{3/2}$ component was found at 134.3 eV: the P2p spectrum is a convolution of the P2p1/2 and P2p3/2 peaks that were resolved, keeping their branching ratio and their difference equal to 0.9 and 1.8 eV, respectively. After uranium sorption (Fig. 7b) the shifting of peaks to higher binding energies were observed. Additionally a new peak was observed at 133.21 eV which could be attributed to P-O-U bond.

U $4f_{7/2}$ spectrum (Fig. 7c) was deconvoluted into two components: the peak corresponding to free uranyl ion occurred at 381.05 eV, and the peak of covalently bonded oxygen and U(VI) occurred at 382.13 eV.

From the above discussion it is clear that, the TBP ligand is grafted onto to CNT and complexation of uranyl ions occurred with the phosphoryl group of tributyl phosphate ligand.

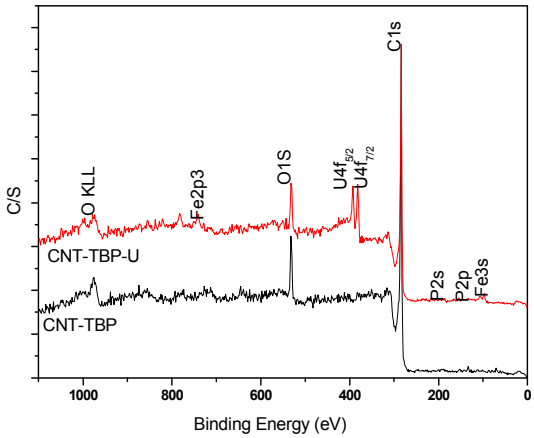

Fig.5 XPS survey scans of plain and U(VI) loaded CNT-TBP systems

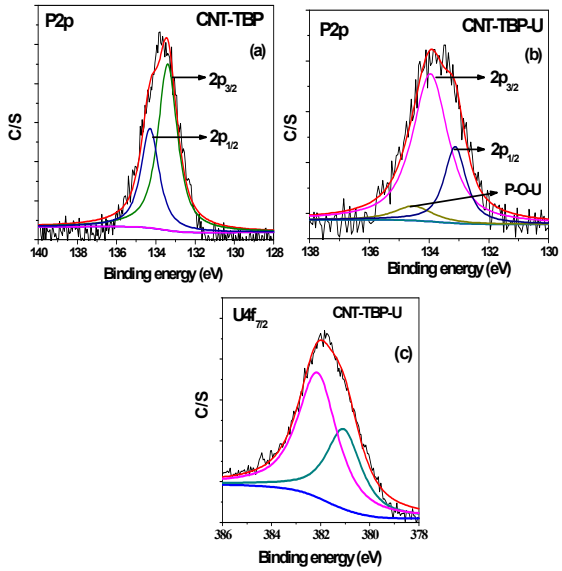

Fig.7 Curve fitted high resolution scans of (a) P 2p of CNT-TBP (b) P2p of CNT-TBP-U (c) U $4f_{7/2}$ of CNT-TBP-U

Table 2. Binding energies(eV) of CNT-TBP before and after Uranium sorption

Adsorbent	C 1s	O 1s	P2p	U 4f5/2	U 4f7/2	Splitting Value
CNT-TBP	284.55	532.02	133.76	-	-	
CNT-TBP-U	283.65	532.47	133.97	392.87	382.15	10.72

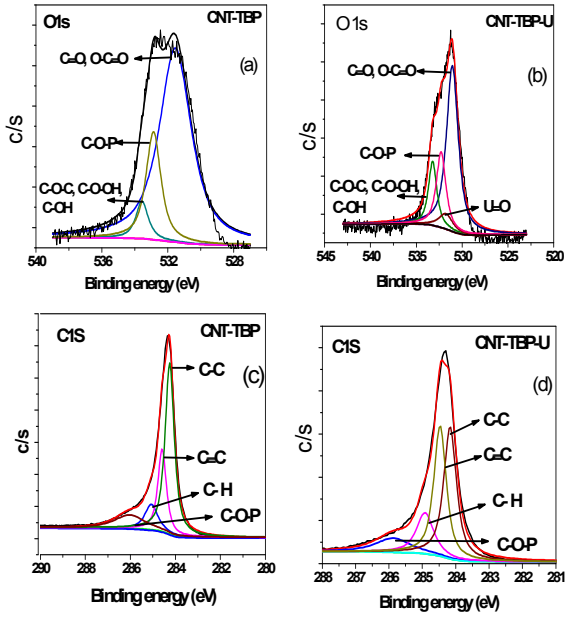

Fig.6 Curve fitted high resolution scans of (a) O1s of CNT-TBP (b) O1s of CNT-TBP-U (c) C1s of CNT-TBP and (d) C 1s of CNT-TBP-U

Table 3. Molecular level binding energies of CNT-TBP and CNT-TBP-U systems

Core levels	CNT-TBP			CNT-TBP-U		
	Binding Energy (eV)	FWHW (eV)	Area	Binding Energy (eV)	FWHW (eV)	Area
C1s	285.06	0.674	1575.04	285.87	1.25	1202.25
	284.58	0.440	3307.22	284.91	0.61	1725.39
	284.25	0.484	7563.98	284.16	0.45	4136.41
	286.03	1.590	1971.61	284.46	0.43	3907.03
O 1s	531.54	2.318	3263.12	531.06	1.51	1944.42
	533.56	0.890	241.96	533.21	1.07	529.58
	532.87	1.073	839.65	531.76	1.79	211.65
				532.29	1.22	717.02
P 2p	133.40	1.184	148.30	133.95	1.41	121.28
	134.30	1.099	82.31	134.52	1.50	12.60
	-	-	-	133.12	0.87	38.65
U 4f7/2	-	-	-	381.05	1.72	990.30
	-	-	-	382.13	1.91	1717.22

Infra red spectra of CNT-TBP before and after U(VI) sorption is shown in Fig.8. It is evident from the figure, after U(VI) sorption, a shift in P=O vibration band to 1110 cm^{-1} was observed. This could be attributed to the coordination of UO_2^{2+}cation with P-O bond of the TBP molecule. The shift of the P=O frequency after U(VI) soprtion was about 82 cm^{-1}, and the magnitude of the frequency shift obtained was consistent with other uranyl complexes with organophosphorus ligands[21,22]. The mode of nitrate complexation to the metal ion can be determined by the separation Δυ of the symmetric υ1, and asymmetric υ2 of NO_2

stretching frequencies[23-25]. A Δυ value > 186 cm^{-1} indicates a bidentate chelate environment, while a Δυ ≤ 115 cm^{-1} indicates a monodentate coordination. It is evident from the spectra that Δυ = 270 cm−1 (υ1 at 1300 cm^{-1} and υ2 at 1530 cm^{-1}) was obtained which indicated a bidentate chelation of nitrate to uranyl ion. Further additional vibration occurred at 950 cm^{-1} which could be assigned to the asymmetric stretching frequency of U=O bond[26]. Based on the above discussions following reaching scheme has been proposed (Scheme 2) for the sorption of Uranyl ion and CNT-TBP

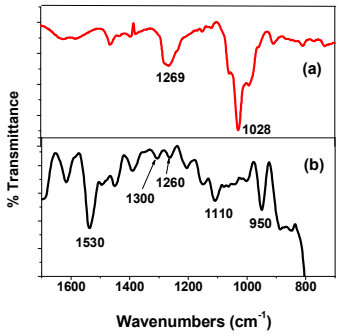

Fig. 8 FTIR scans of (a) CNT-TBP (b) CNT-TBP-U

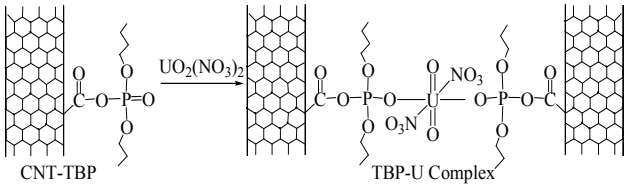

Scheme 2. Schematic representation of U(VI) loading on CNT-TBP

3.3 Effect of initial pH on sorption

The initial pH of the solution containing 100 mg/l of uranyl ions was varied from 2 – 8 and equilibrium experiments were carried out (Fig.9). The amount of uranyl ions adsorbed increased from pH 4 to pH 6 and further increase in pH resulted in the decreased sorption. The adsorption trends observed over the pH range studied could be assigned to the distribution of various uranyl species. It is well known that at pH values ≤ 3, UO_2^{2+} is the predominant species[11] and in the pH range of 4.0 – 9.0, hydrolysis of U(VI) occurred and other uranyl complexes, including $UO_2(OH)^+$, $(UO_2)_2(OH)_2^{2+}$ and $(UO_2)_3(OH)_5^+$ [27] were prevalent. However at pH values > 7.0 anionic uranyl species $(UO_2)_3(OH)_7^-$ also coexisted[28]. The lower adsorption rate of uranyl ions at pH values < 4 could be attributed to the competition of protons for the active surface of CNTs. Thus adsorption of uranyl ions was found to be maximum around pH 5 for CNT-TBP and at pH 6 for CNT-OX and CNT plain. At pH > 7 negatively charged uranyl complexes were repelled by negative surface charge of the sorbent resulting lower capacity. Due to functionalization of TBP ligand onto CNTs the amount of Uranyl adsorbed was found to be higher for CNT-TBP compared to plain and oxidized CNTs.

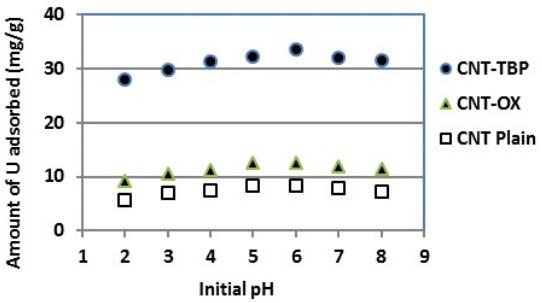

Fig.9 Effect of initial pH on sorption of U(VI) with CNT-Plain, CNT-OX and CNT-TBP

3.4 Kinetics of sorption

The adsorption of an aqueous solution containing U(VI) on CNT-Plain, CNT-OX and CNT-TBP was carried out at pH at pH 5.0 ± 0.1 to investigate the kinetics of sorption. Figure 10a showed that the adsorption process on various sorbents for U(VI) removal. A contact time of 3.0 h was sufficient for adsorption of uranyl ions onto CNT-TBP to reach equilibrium. However, for CNT-Plain and CNT-OX reach equilibrium at 3.5 h. Kinetics of U(VI) adsorption onto all the sorbents prepared were modelled using Lagergren model[29] or pseudo first order, second order[30] and pseudo second order[31] shown in Eqns (2) – (4) respectively.

$$\log(q_e - q_t) = \log q_e - \frac{k_L}{2.303}t \quad (2)$$

$$\frac{1}{q_t} = \frac{1}{q_e} + k_2 t \quad (3)$$

$$\frac{t}{q_t} = \frac{1}{k_2 q_e^2} + \frac{t}{q_e} \quad (4)$$

where k_L is the Lagergren rate constant of sorption (min^{-1}); k_2 the second-order rate (g/mg/min) and k_2' the pseudo-second-order rate constant of sorption (g/mg/min); qe and qt are the amounts of uranyl ion sorbed (mg/g) at equilibrium and at a given time t, respectively. The kinetic model plots are shown in Figs. 10b – 10d. From Table 4, it is evident that among various models, pseudo second order plot of t/q_t *Vs* t (Fig. 10 d) yielded a regression coefficient > 0. 978. Thus, it could be concluded that the adsorption of uranyl ions with the prepared sorbents followed pseudo second order kinetic model. Further, Weber and Morris model[32] describes the intraparticle diffusion between the sorbent and sorbate. This model correlates the amount of the solute adsorbed and the intraparticle diffusion rate constant (k_{int}) given by the equation given below:

$$q_t = k_{int}\sqrt{t} + C \quad (5)$$

It is evident from Fig. 8e that the plot of q_t *Vs* $\sqrt{t}$ yields an intercept and this confirms that in addition to intraparticle

diffusion, chemisorptions could also be involved. The values obtained from this model are presented in Table 4.

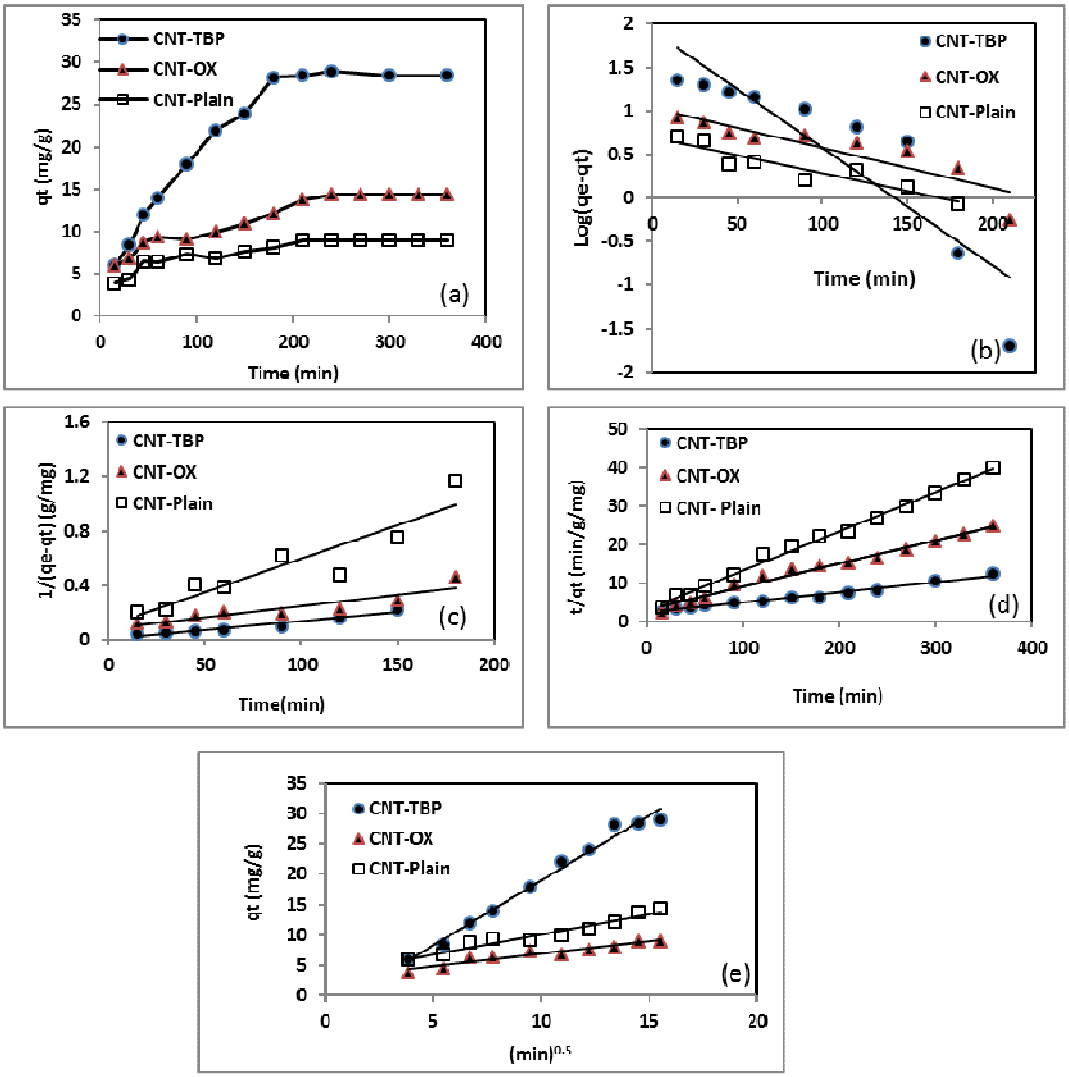

Fig. 10a. Equilibration time b. Pseudo First order kinetics c.Second Order kinetics d. Pseudo Second Order kinetics and e. Web-Morris model of CNT-TBP and U(VI)

Table 4. Kinetic rate constants on the sorption of U(VI) by various CNTs

Adsorbent	Pseudo First Order		Second Order		Pseudo Second Order		Web-Morris Model	
	K_1 (min^{-1})	R^2	k_2 (mg/g/min)	R^2	k_2' (mg/g/min)	R^2	k_{int} (mg/g/$min^{0.5}$)	R^2
CNT-Plain	0.877	0.870	0.001	0.844	0.0031	0.994	0.670	0.945
CNT-OX	0.004	0.803	0.005	0.859	0.0012	0.981	0.409	0.906
CNT-TBP	0.013	0.800	0.001	0.926	0.0003	0.978	2.147	0.986

3.5 Equilibrium studies

Sorption data of uranyl ions with various CNTs were modelled using commonly used isotherms (Fig.11). Langmuir model describe the monolayer adsorption and equivalency of the surface adsorption sites. The linearised Langmuir model [32] could be expressed as

$$\frac{1}{q_e} = \frac{1}{q_0 C_e K_L} + \frac{1}{q_m} \qquad (6)$$

Where, C_e is the equilibrium concentration (mg/L) and q_e is the amount of U(VI) sorbed (mg/g) at equilibrium. The empirical constants b and q_m denote the energy of adsorption and maximum adsorption capacity, respectively. The results obtained for the various model parameters are listed in Table 5. The langmuir adsorption capacity of the prepared adsorbents towards uranyl ions were in the order of CNT-TBP > CNT-OX > CNT-Plain. The adsorption capacity of CNT-TBP was found to be 2.5 times higher than plain CNT. Complexing ability of TBP ligand towards U(VI) resulted in increased sorption capacity. Comparison of the prepared adsorbents with other functionalized CNTs reported in literature is listed in Table 6. For example, the capacity obtained for CNT-TBP is higher than plain oxidized MWCNT[28] (43.32 mg g^{-1}), diglycolamide functionalized MWCNTs[334] (133.7 mg g^{-1}), Carboxymethyl cellulose grafted CNT[35] (112.0 mg g^{-1}), imine functionalized carbon spheres[36] (113 mg/g) and palm shell activated carbon[27] (51.81 mg g^{-1}). A comparison of the adsorption capacities of various functionalized CNTs are given in Table 6.

The linear Freundlich model is represented below[29]

$$\log q_e = \frac{1}{n_F}\log C_e + \log K_F \qquad (8)$$

The K_F and n_F represent the sorption intensity and sorption capacity respectively. The values of "n_F" ranging between 1 to 10 indicates a good adsorbent. In the present study (Table 5) the 'n' values ranged between 1.445 to 1.835. This signifies the good adsorption capability of CNT, CNT-OX and CNT-TBP towards uranyl ion.

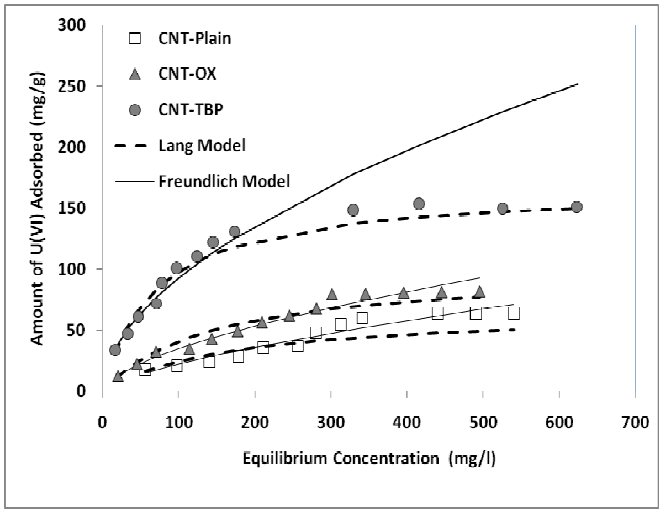

Fig.11 Adsorption isotherms of various adsorbents with U(VI)

Table 5. Isotherm Parameters of CNT-Plain, CNT-OX and CNT-TBP

Adsorbent	Langmuir Model			Freundlich Model		
	q_{max} (mg g^{-1})	b (L mg^{-1})	R^2	K_F (L g^{-1})	n_F	R^2
CNT-Plain	66.66	0.0057	0.845	0.918	1.445	0.926
CNT-OX	100.00	0.0223	0.985	2.138	1.645	0.981
CNT-TBP	166.66	0.0142	0.972	7.533	1.835	0.964

Table 6. Comparison of the maximum adsorption capacities of various functionalized CNTs towards U(VI) removal

Adsorbent	MaximumAdsorption Capacity(mg/g)	Reference
Plasma functionalized MWCNT	66.16	40
Oxidized MWCNT	43.30	28
Diglycolamide functionalized MWCNT	133.70	34
Oxidized MWCNT	33.30	10
Carboxymethylcellulose functionalized CNT	112.00	35
Oxidized MWCNT	45.90	11
Graphene Oxide-CNTs	100.0	41
Amidoxime-CNTs	145.0	42
Montmorillonite@C	20.76	43
$CoFe_2O_4$/MWCNTs	212.7	44
CNT-Plain	66.66	Present Work
CNT-OX	100.00	Present Work
CNT-TBP	166.66	Present Work

3.6 Thermodynamic studies

The feasibility of adsorption was elucidated using thermodynamic parameters like ΔG°, ΔH° and ΔS° which were calculated using the adsorption data. Initially, the constant *Kc,* was calculated the ratio of U(VI) adsorbed onto the sorbent

C_A(g/L) to that in aqueous phase at equilibrium C_e (g/l) given by the following equation

$$K_C = \frac{C_A}{C_e} \quad (10)$$

Then, ΔG° was determined using the eqn.11

$$\Delta G^\circ = -RT \ln Kc \quad (11)$$

where R is the gas constant and T is the temperature in Kelvin. Further, ΔSº and ΔHº was determined using Van't Hoff equation (12):

$$\log Kc = \frac{\Delta S^\circ}{2.303} - \frac{\Delta H^\circ}{2.303RT} \quad (12)$$

A plot of log K_c vs. 1/T was obtained for uranyl ions and CNT-TBP system (Fig.12). The thermodynamic parameters namely ΔH° and ΔS° were determined from the slope and intercept, respectively. Table 7 lists the values obtained for various thermodynamic parameters. The negative Gibbs free energy indicated the effectiveness and spontaneity of the sorption process. The endothermic nature of the adsorption process is revealed by the positive enthalpy (ΔH°) values. Positive entropy (Δ*S*°) values could be due to the dehydration of uranyl ions during adsorption.

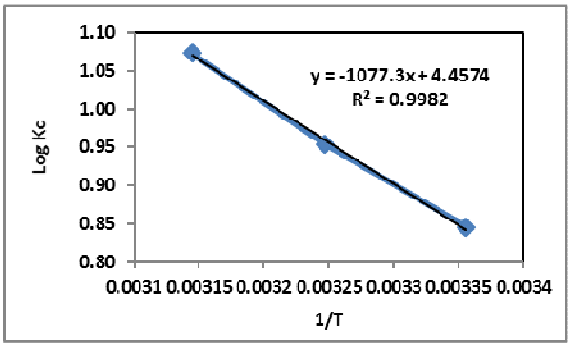

Fig.12 Thermodynamic studies of CNT-TBP and U(VI) systems

Table 7. Thermodynamic parameters of CNT-TBP and U(VI)

T (K)	Ce (g/l)	Kc	ΔG (KJ/mol)	ΔS (J/mol)	ΔH [kJ/(mol/K)]
298	12.5	7.00	-4.81		
308	10.0	9.00	-5.63	10.26	20.62
318	7.8	11.82	-6.53		

3.7 Desorption and Recyclability Studies

After adsorption of uranyl ions using CNT-TBP as sorbent, desorption studies of uranium were conducted. It was found that .1 M HCl efficiently stripped adsorbed uranium ions. The amount of uranyl ions adsorbed and desorbed for three consecutive cycles using CNT-TBP as sorbent is shown in Fig. 13. A decreased U(VI) uptake in the order of 11 and 20%, were observed at the end of 1st and 2nd cycle respectively. Using ordered mesoporous carbon[12] and functionalized activated carbon fibers[9] as adsorbents similar results were observed.

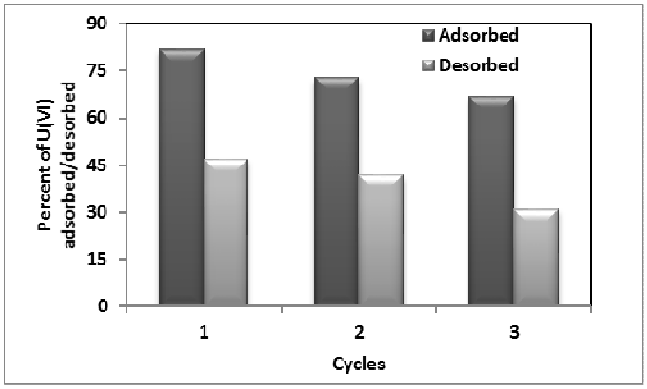

Fig.13 Desorption and Recyclability Studies

4. Conclusions

Chemical vapour deposition technique was used to synthesize carbon nanotubes indigenously using ferrocene and benzene as hydrocarbon source. Ferrocene acted as a floating catalyst and hydrocarbon source as well. Efficient functionalization were carried out by oxidation with nitric acid and grafting tributyl phosphate ligand. FTIR and XPS studies confirmed the presence of phosphoryl group on CNT-TBP. Pseudo second order model was found to fit the experimental data. A Langmuir adsorption capacity of 166.6mg/g was obtained for CNT-TBP with high regression coefficient. Efficient complexation of U(VI) and TBP ligand resulted in high sorption capacity compared to CNT and CNT-OX. The spontaneity of the reaction was revealed by thermodynamic studies and the desorption and recyclability studies were carried out for 3 cycles. The FTIR and XPS showed the involvement of phosphoryl group of the TBP ligand towards the interaction of uranium.

Acknowledgements

The funding received from Board of Research in Nuclear Sciences, Department of Atomic Energy, Mumbai, India (Ref. No. 2013/36/57-BRNS/2482) to carry out this work is gratefully acknowledged.

References

1 K. Sakr, M. S. Sayed and M. B. Hafez, *J. Radioana.l Nucl. Chem.*, 2003, **256**, 179.
2 T. Ozdemir and A. Usanmaz , *Prog. Nucl. Energ.,* 2009, **51**, 240.
3 B. Allard, U. Olofsson and B. Torstenfelt, *Inorg. Chim. Acta.*, **1984**, 94, 205.
4 G.M. Naja and B.Volesky, *Toxicity and sources of heavy metals of Pb, Cd, Hg, Cr, As and radionucleides in the environment*, CRC Press, Taylor and Francis Group, USA, 2009, 16.
5 WHO, *Guidelines for Drinking Water Quality*, Geneva, 2nd edn, 1998, 283.

6 P. D. Bhalara, D. Punetha and K. Balasubramanian, *J. Environ. Chem. Eng.*, 2014, **2**, 1621.
7 M. Caccin, F. Giacobbo, M. Da Ros, L. Besozzi and M. Mariani, *J. Radioanal. Nucl. Chem.*, 2013, **297**, 9.
8 A. M. A. Morsy and A. E. M. Hussein, *J. Radioanal. Nucl. Chem.*, 2011, **288**, 341.
9 S. Mishra, J. Dwivedi, A. Kumar and N. Sankararamakrishnan, *RSC. Adv,* 2015,**5,** 33023.
10 Y. Sun, S. Yang, G. Sheng, Z. Gua and X. Wang, *J. Environ. Radioact.*, 2012, **105**, 40.
11 A. Schierz and H. Zanker, *Environ. Pollut.*, 2009, **157**, 1088.
12 B.-W. Nie, Z.-B. Zhang, X.-H. Cao, Y.-H. Liu and P. Liang, *J. Radioanal. Nucl. Chem.*, 2012, **295**, 663.
13 P. Giridhar, K. A. Venkatesan, T. G. Srinivasan and P.R. Vasudeva Rao, *J. Radioanal. Nucl. Chem.,* 2005, **265**, 31.
14 N. Sankararamakrishnan, D. Chauhan, J. Dwivedi, *Chem. Eng. J* 2016, **284**, 599.
15 B. Chen, Z. Zhu, J. Ma, Y, Qiu and J. Chen, *J. Mater. Chem*., 2013, **1**, 11355.
16 M. Alibrahim and H. Shlewit , Period. polytech. 2007, **51**, 57.
17 V. Datsyuk, M. Kalyva, K. Papagelis, J. Parthenios, D. Tasis, A. Siokou, I. Kallitsisc and C. Galiotis*, Carbon*, 2008, **46**, 833.
18 A. Rossi, F. M. Pirasa, D. Kim, A. J. Gellman and N.D. Spencer, **Tribol. Lett.,** 2006, **23**, 197.
19 S. Van den Berghe, F. Miserque, T. Gouder, B. Gaudreau and M. Verwerft, *J. Nucl. Mater*., 2001, **294**, 168.
20 S. Chen, J. Hong, H. Yang and J. Yang, *J. Environ. Radioact.*, 2013, **126**, 253.
21 L.L. Burger, Physical properties, Science and Technology of Tributyl phosphate (Schulz WW, Navratil JD, eds.), CRC Press: Boca Raton, Florida, 1984, 26.
22 D. F. Peppard and J. R.Ferraro, *J. Inorg. Nucl. Chem*., 1959, **10**, 275.
23 B.M. Gatehouse, S. E. Livingstone and R.S. Nyholm, *Chem. Soc.* 1959, 4222.
24 N. F. Curtis and Y.M. Curtis, *J. Inorg. Chem*., 1965, **4** , 804.
25 J.R. Ferraro and D.F. Peppard, *Nucl. Sci. Eng*., 1963, **16**, 389.
26 K.W. Bagnall and M.W. Wakerley, *J. Inorg. Nucl. Chem.,* 1975, **37**, 329.
27 G. Wang, J. Liu, X. Wang, Z. Xie and N. Deng, *J. Hazard. Mater*., 2009, **168,** 1053.
28 M. Wang, J. Qiu, X. Tao, C. Wu, W. Cui, Q. Liu, S. Lu, *J. Radioanal. Nucl. Chem*., 2011, **288**, 895.
29 S. Lagergren, *K. Sven. Vetenskapsakad. Handl.*, 1898, **24**, 1–39.
30 Y. S. Ho, D. A. J. Wase and C. F. Forster, *Environ. Technol.*, 1996, **17**, 71.
31 Y. S. Ho and G. McKay, *Advances in Adsorption Separation Science and Technology*, South China University of Technology Press, Guangzhou, 1997, 257.
32 W. J. Weber and J. C. Morris, *J. Sanit. Eng. Div., Am. Soc. Civ. Eng.*, 1963, **89**, 31.
33 I. Langmuir, *J. Am. Chem. Soc.*, 1918, **40**, 1361.
34 A. K. S. Deb, P. Ilaiyaraja, D. Ponraju and B. Venkatraman, *J. Radioanal. Nucl. Chem.*, 2012, **291**, 877.
35 D. Shao, Z. Jiang, X. Wang, J. Li and Y. Meng, *J. Phys. Chem. B*, 2009, **113**, 860.
36 P. S. Dubey, D. A. Dwivedi, M. Sillanpaa, Y.-N. Kwon and C. Lee, *RSC Adv.*, 2014, **4**, 46114.
37 Z.-J. Yi, J. Yao, J.-S. Xu, M.-S. Chen, W. Li, H.-L. Chen and F. Wang, *J. Radioanal. Nucl. Chem.*, 2014, **301**, 695.
38 N. Sankararamakrishnan, A. Dixit, L. Iyengar and R.Sanghi, Bioresource Technol, 2006, **97**, 2377.
39 H. M. F. Freundlich, *J. Phys. Chem.*, 1906, **57**, 385.
40 M. Song, Q. Wang and Y. Meng, *J.Radio.Nucl*., 2012, **293**, 899.
41 Z.Gu, Y. Wang, J. Tang, J.yang, J.Liao, Y. Yang and N. Liu, *J. Radioanal. Nucl. Chem*., 2015, **303**, 1835.
42 Y. Wang, Z. Gu, J. Yang, J. Liao, Y. Yang, N. Liu, J. Tang, *Appl. Surf. Sci.,* 2014*,* **320**, 10.
43 R. Zhang, C. Chen, J. Li, X. Wang, *Appl. Surf. Sci*., 2015, **349**, 129.
44 L. Tan, Q. Liu, X. Jing, J. Liu, D. Song, S. Hu, L. Liu, J. Wang, *Chem. Eng. J*, 2015, **273**, 307.

Efficient method for grafting tributylphosphate onto carbon nanotubes (CNT-TBP) is described. CNT-TBP exhibited excellent adsorption towards U(VI) ions.